Title
DISLOCATION SUBSTRUCTURE IN QUENCHED ALUMINUM SINGLE CRYSTALS

Author
Strudel, J.L.

Publication Date
1963-06-01

UCRL-10793

University of California

Ernest O. Lawrence Radiation Laboratory

DISLOCATION SUBSTRUCTURE IN QUENCHED ALUMINUM SINGLE CRYSTALS

Berkeley, California

DISCLAIMER

UCRL-10793
UC-25, Metals, Ceramics
and Materials
TID-4500 (19th Ed.)

UNIVERSITY OF CALIFORNIA

Lawrence Radiation Laboratory
Berkeley, California

Contract No. W-7405-eng-48

DISLOCATION SUBSTRUCTURE IN QUENCHED ALUMINUM SINGLE CRYSTALS

J. L. Strudel

(Master's Thesis)

June 1963

Printed in USA. Price $1.00. Available from the
Office of Technical Services
U. S. Department of Commerce
Washington 25, D.C.

Table of Contents

UCRL-10793

DISLOCATION SUBSTRUCTURE IN QUENCHED ALUMINUM SINGLE CRYSTALS

Jean-Loup Bernard Strudel

Lawrence Radiation Laboratory
University of California
Berkeley, California

June 1963

ABSTRACT

Observations have been made by transmission electron microscopy of thin foils of high purity aluminum single crystals quenched from 651°C into water at 0°C. Loops of 250 Å diameter have been found lying on (111) planes. Electron diffraction contrast experiments using single crystals of [111] orientation have shown that the loops are 99% of the Frank sessile type. Single crystals of [110] orientation have been used to study interactions between glissile dislocations and Frank sessile loops. When a moving dislocation came close to a loop the stacking fault was destroyed and the loop often became attached to the moving dislocation causing it to glide prismatically to the surface of the foil.

I. INTRODUCTION

At any temperature different from 0°K, vacant sites are in equilibrium in the crystalline lattice of metals. The concentration of vacancies is strongly temperature dependent and is given by the approximate relation:

$$C_v = \exp\left(\frac{-U_{fv}}{kT}\right)$$

where C_v is the fraction of the total number of lattice sites that are not occupied by an atom and U_{fv} is the energy of formation of a vacancy which is of the order of 0.76 eV for aluminum.[1] As a consequence, when a pure metal is rapidly cooled from a high temperature, vacancies are quenched in. Vacancy concentrations of the order of 10^{-4} can be obtained by quenching aluminum samples from 600°C into water at 0°C.

As first observed by Bradshaw and Pearson,[2] Federighi,[3] De Sorbo and Turnbull,[4] quenching increases electrical resistivity. If it is assumed that this increase is due to excess vacancies, then an estimate of U_{fv} can be made from quenching experiments.

Defects produced by quenching also affect mechanical properties. An increase in yield strength has been observed after quenching and aging of pure metals.[5-7]

Direct observation of thin foils of quenched metals by transmission electron microscopy has revealed the presence of aggregates of vacancies. Frank (1950)[8] suggested that dislocation loops might be produced by the collapse of discs of vacancies. This idea was elaborated in 1950 by Seitz[9] who suggested that prismatic dislocation loops would be produced after quenching and that, suitably arranged, they might constitute the substructure of crystals.

This theory has been developed and many experimental results have been reported and summarized in a review article by Kuhlmann-Wilsdorf and Wilsdorf.[1]

The exact mechanism of loop formation is not completely elucidated yet. The authors of this latter article suggested that loops were formed by collapse of three-dimensional aggregates containing 20 to 1,000 vacancies.

Stacking fault energy is expected to play an important role in determining the choice between three different kinds of dislocation configurations that can form in FCC metals by condensation of vacancies:

(1) Stacking fault tetrahedra with stair-rod dislocations at each edge are observed in metals of low stacking fault energy. Examples have been obtained in quenched gold by Silcox and Hirsch.[10]

(2) In metals of high stacking fault energy like aluminum, vacancies may condense to form perfect prismatic dislocation loops (Burgers vector $\frac{1}{2}$ [110] not lying in the plane of the loop) as first suggested by Kuhlmann-Wilsdorf[7] and reported by Hirsch et al.[11]

(3) Although Frank sessile loops (Burgers vector $\frac{1}{3}$ [111] lying perpendicular to the plane of the loop) are energetically unstable in aluminum above a critical size, Vandervoort and Washburn,[12] Segall and Cotterill,[13] and Yoshida et al.[14] have observed this type of loop in high purity aluminum. Their presence has been explained by Saada:[15] the activation energy for the nucleation of a Shockley partial is too high to allow conversion to take place even in metals of high stacking fault energy.

Recent experimental results and their interpretation by Yoshida et al.[16] have definitely proved that up to 90% of the loops are of the stacking fault type in high purity aluminum quenched from 600°C into 0°C water. Some of the perfect loops that are present may have been formed by interaction of an imperfect loop with a moving dislocation.

The presence or absence of stacking fault fringes[17] has often been taken as the sole criterion for discriminating between Frank sessile and

perfect prismatic loops. This method is applicable only to large loops on inclined planes with diameters at least equal to the extinction distance for the metal and the diffracting planes under consideration. The extinction distance is of the order of 600 Å in aluminum with the (111) reflection. Therefore, loops smaller than 500 Å in diameter lying on inclined planes will not be clearly identifiable. Until now experiments have not been done on single crystals to elucidate the situation.

The purpose of the present experiments is twofold:

(1) To determine the Burgers vector of small loops in the size range 100 to 250 Å in quenched high purity aluminum.

(2) To investigate the interaction of moving dislocations with small Frank sessile dislocation loops.

Both of these objectives were facilitated by the use of single crystal specimens having (111) or (110) plane parallel to the surface. With these orientations the diffraction conditions are favorable to the determination of the Burgers vector. Sets of loops will become invisible whenever their Burgers vector lies in the reflecting plane, i.e., whenever $\vec{g}.\vec{b} = 0$. Table I gives the values of $\vec{g}.\vec{b}$ for the most common diffraction conditions.

For reasons of convenience Thompson tetrahedron (fig. 15) and Thompson's notation[18] will be used when dealing with geometrical problems and indices notation when dealing with problems of contrast.

If the [111] orientation is used, the following situation can be expected:

-loops of type $\frac{1}{2}[\bar{1}10]$, $\frac{1}{2}[\bar{1}01]$ and $\frac{1}{2}[0\bar{1}1]$ will always be in contrast whatever the diffracting plane, as shown in Table I.

-loops of type $\frac{1}{2}[110]$, $\frac{1}{2}[101]$ and $\frac{1}{2}[011]$, on the contrary, will seem to behave like loops of type $\frac{1}{3}[11\bar{1}]$, $\frac{1}{3}[1\bar{1}1]$ and $\frac{1}{3}[\bar{1}11]$, i.e., both sets

TABLE I

Values of $\vec{g}.\vec{b}$ for the Most Common Diffraction Conditions When Using Single Crystals of Orientation [111] or [110].

	[111] orientation			[110] orientation		
Operating diffraction / Burgers vector	$\bar{2}20$	$\bar{2}02$	$0\bar{2}2$	$\bar{1}11$	$1\bar{1}1$	002
$\frac{1}{3}[\bar{1}11]$	$\frac{4}{3}$	$\frac{4}{3}$	0	1	$-\frac{1}{3}$	$\frac{2}{3}$
$\frac{1}{3}[1\bar{1}1]$	$-\frac{4}{3}$	0	$\frac{4}{3}$	$-\frac{1}{3}$	1	$\frac{2}{3}$
$\frac{1}{3}[11\bar{1}]$	0	$-\frac{4}{3}$	$-\frac{4}{3}$	$-\frac{1}{3}$	$-\frac{1}{3}$	$-\frac{2}{3}$
$\frac{1}{3}[111]$	0	0	0	$\frac{1}{3}$	$\frac{1}{3}$	$\frac{2}{3}$
$\frac{1}{2}[110]$	0	-1	-1	0	0	0
$\frac{1}{2}[101]$	-1	0	1	0	1	1
$\frac{1}{2}[011]$	1	1	0	1	0	1
$\frac{1}{2}[\bar{1}10]$	2	1	-1	1	-1	0
$\frac{1}{2}[\bar{1}01]$	1	2	1	1	0	1
$\frac{1}{2}[1\bar{1}0]$	-1	1	2	0	1	1

of loops will appear in contrast and become invisible under the same diffraction conditions. Their Burgers vector lie in the same vertical plane.

However, assuming that the loops are of perfect prismatic type, $\frac{5}{6}$ of them should always be in contrast position and only $\frac{1}{6}$ of them should appear or disappear when changing the diffraction conditions. On the contrary, if the loops are of Frank sessile type, the change in diffraction conditions affect $\frac{2}{3}$ of those that are visible (the $\frac{1}{3}$ [111] set is always invisible); $\frac{1}{3}$ of them will disappear and another $\frac{1}{3}$ will become visible.

If the [110] orientation is used, similar differences can be expected. Table I shows that the Frank sessile loops will always be in contrast whatever the diffraction conditions, whereas perfect prismatic loops will not.

The above considerations on contrast are only reliable when dealing with loops lying on (111) planes. However, perfect prismatic loops are mobile on their glide cylinder and are often observed to rotate.[1,31] If they tend to be in pure edge orientation, they are easily distinguishable from Frank sessile loops by inspection of the habit plane as shown in figures 16 and 17. See loops a and b on figures 1a, 2a, 3 and the rotation of S in figure 14a into S' in figure 14b.

In order to determine the habit plane and the Burgers vector of the observed defect an accurate orientation of the foil is required and can be carried out by direct construction on the picture itself. Note that the slip traces on figures 9 and 10 intersect each other although they should be parallel if the plane of the foil was exactly perpendicular to the [110] direction. The line bisecting the angle between the slip traces is the projection of the $[\bar{1}10]$ direction. Loops lying on the $[\bar{1}11]$ are seen edge on. This indicates that the $[\bar{1}11]$ direction is lying in the plane of the foil.

From these two indications, it is possible to determine the orientation of the crystal to within about $\pm 1°$.

A convenient way to describe the orientation of the pictures is to represent the projection of a Thompson tetrahedron[18] in the direction of observation. This representation is used on all the figures.

A single crystal of [110] orientation is also more suitable for studying interaction between Frank sessile loops and moving dislocations. The slip traces of moving dislocations are broader since the angle between the [110] and the [111] directions is 35°16' instead of 70°32' as in the [111] orientation and all the Frank sessile loops are visible at the same time whatever the diffraction conditions are (Table I).

II. EXPERIMENTAL PROCEDURES

1. Single crystals 20 cm x 2.5 cm x .05 cm were grown from 99.999% pure aluminum in a graphite mold packed with spectroscopic, dessicated graphite powder and under vacuum.

2. Mechanical polishing was found necessary to remove the thick alumina coating created unavoidably during the process of growing the single crystal. No chemical or electrochemical polishing process seemed to be satisfactory. A complete and uniform removal of the oxide layer was required for the next step.

3. Chemical polishing was then carried out on the 0.5 mm thick specimen in order to thin it down to 0.25 mm (square specimen 2.5 cm x 2.5 cm).

Composition of the polishing solution:

Phosphoric acid (86%)	800 cm^3
Sulfuric acid (96%)	120 cm^3
Nitric acid (70%)	80 cm^3

used at 95°C, removes 8 to 10 μ/min.

4. The 0.25 mm thick sample was annealed in air for 24 hours at 640°C and furnace cooled.

5. The sample was heated for 20 min. at 651°C in the quenching furnace and then quenched into water at 2°C. Rapid quenching was achieved by having the travel distance from the hot zone of the furnace to the quenching bath as short as possible and by using a 1-meter-deep quenching bath into which the specimen was pulled by a weight of four pounds acting on the specimen holder.

6. The specimen was then aged for one hour at room temperature. This step allowed the vacancies to diffuse through the lattice and cluster to form loops.[23]

7. Electrochemical polishing[24] at 4°C was performed in a stainless steel beaker cooled with ice. The window method was used with a slightly modified perchloric acid-ethyl alcohol solution:

Ethyl alcohol	(190 proof)	120 cm^3
Perchloric acid	(70%)	30 cm^3
Butylcellosolve		10 cm^3

The latter ingredient increased the viscosity of the solution allowing polishing to be carried out at 4°C instead of at -30°C or -40°C.

Applied voltage:	28 volts
Current density:	0.1 amp/cm^2

Near the end of the thinning process the voltage was decreased to 12 volts and the current switched on and off. Flakes were obtained which were washed abundantly with 200 proof alcohol.

8. Specimens were mounted on 75 mesh copper grids and observed by transmission electron microscopy in a Siemens Elmiskop I operated at 100 kV. Use of the stereo-tilting stage enabled various diffraction contrast conditions to be obtained. Selected area diffraction patterns were taken from 1.5 μ^2 areas.

III. RESULTS AND INTERPRETATION

A. General Features

As in polycrystalline samples, colonies of loops were found bounded by subgrain boundaries which were surrounded by loop-free areas. The three-dimensional dislocation network that existed in the crystal prior to quenching acted as a powerful sink[25] for excess vacancies. The average size of the loops after quenching from 651°C into water at 0°C was 250 Å. Loops somewhat larger than the average size were found on the edges of the colonies.[26] This is consistent with previous results obtained from polycrystalline samples and with the generally accepted theory: there are only three ways excess vacancies can be removed:

1. by migration to an external surface or to grain boundaries,

2. by precipitation on edge dislocations or on screw dislocations which are transformed into helixes,[27-28]

3. by clustering to form small voids that later collapse into dislocation loops.[1]

Figures 4 and 5 show a typical structure. The foil is 5000 Å thick, the loop density is about $8 \times 10^{13}/cm^3$, and the average diameter of the loop is 500 Å. Higher loop densities are shown in figures 1a, 2a and 3. Foil thickness is 1000 Å with a loop density of $6 \times 10^{14}/cm^3$ and an average loop diameter of 250 Å. Assuming that all the excess vacancies are represented by the loop vacancy concentrations prior to quenching were 10^{-4} and 2×10^{-4} respectively for these areas.

Dislocation movements were often observed. Figures 6, 7, 8, 9 and 10 are sequences of the same area of the specimen after the passage of moving dislocations.

B. Determination of the Burgers Vector of the Loops

Because of the size of the loops, the observed images cannot be interpreted directly from the results obtained by Howie and Whelan[17,19,20] and by Gevers[21] about the images of isolated dislocations or large dipoles. Those interpretations assume that the stress field of the dislocation is not altered by the presence of any other defect. Dealing with loops of 250 Å diameter, the stress field about a point of the dislocation is affected by the presence of the rest of the loop and the interaction between the stress fields of two opposite points on the loop cannot be neglected. Therefore, the observed shape of the image has to be considered more representative of the stress field of the dislocation loop than of the actual dislocation line. However, it is still true that diffraction contrast for a small loop will almost vanish when $\vec{g}.\vec{b} = 0$. Also, imperfect loops of Burgers vector $\frac{a}{3}\langle 111\rangle$ must lie in the {111} planes, whereas perfect loops with Burgers vector $\frac{a}{2}\langle 110\rangle$ will probably rotate toward the pure edge orientation.

For small loops having a diameter of less than 500 Å, stacking fault fringes cannot always be observed because the size of the loop is comparable to the spacing of the fringes. Also, the shape of the image which is caused by the stress field of the dislocation loop may be quite different from the real shape of the defect. The hexagonal shape is generally lost below a diameter of 400 Å. The Burgers vector $\vec{b}$ of the loop can only be determined by relying on the value of $\vec{g}.\vec{b}$:

- whenever $\vec{g}.\vec{b} = 0$ the set of loops of Burgers vector $\vec{b}$ will be in strong contrast,
- whenever $\vec{g}.\vec{b} = 0$ the set of loops will almost vanish if they are pure edge.

This is illustrated by figures 1a, 1b, 2a, 2b and 3 taken from the same area of a (111) specimen. The loops belong to three different sets that become visible and vanish according to the change in diffraction conditions. This observation is consistent with the assumption that the loops all lie on the {111} planes and that those on the plane parallel to the foil surface are always out of contrast. All the loops that appear to have the same habit plane vanish together. This could only happen if the great majority of the loops are of the Frank sessile type having $\frac{a}{3}$ {111} Burgers vectors. If appreciable numbers of $\frac{a}{2}$ <110> loops were present, the situation would be much more complex. There would be at least six different sets of loops distinguishable under various diffraction conditions. If they lay on {111} planes, then only one third of the loops on each of two {111} planes would go out of contrast together.

A few loops like those at a and b which are not out of contrast for any of the three diffraction conditions are probably perfect loops with Burgers vector $\frac{a}{2}$ <110>.

The distribution of the loops of a certain set across the specimen seems to be uniform and at random. Notice that the thickness of the specimen decreases towards the top of the figure. On the other hand, the distribution of loops between the three visible sets was often unequal. For example, in figs. 1-3 the relative numbers of loops on the three {111} planes were:

loops on $(\bar{1}11)$ $\simeq$ 150 (or plane c)
loops on $(1\bar{1}1)$ $\simeq$ 75 (or plane a)
loops on $(11\bar{1})$ $\simeq$ 30 (or plane b)

This unequal distribution between the three {111} planes may be due to a stress-sensitive nucleation of the loops. Stress fields induced during quenching might influence the critical stage during which a cluster of vacancies collapses to form a loop.

According to these results, the percentage of loops of Frank sessile type is very high: 99% or more, which agrees with earlier experiments[16] in which specimens were quenched from lower temperatures.

C. Interactions Between Frank Sessile Loops and Glissile Dislocations

Interaction between dislocation loops or stacking fault tetrahedra and moving dislocations have been observed by Kuhlmann,[31] Silcox[10] and Hirsch[11,29] et al. and a general theory has been developed by Saada and Washburn.[30] For the case of an $\frac{a}{2}$ <110> dislocation that intersects a loop of Burgers vector $\frac{a}{3}$ <111> two different cases can be considered:

First, assume that the loop lies on one of the glide planes of the moving dislocation (fig. 19). It can split into two Shockley partials in the plane of the stacking fault that will sweep away the fault. The moving dislocation is connected by two nodes to curved dislocation segments. This configuration may act as a strong anchor point unless high stresses or image forces cause one of the segment to move, in which case prismatic glide takes place.

The second case occurs when the loop is not lying on either of the glide planes of the dislocation (fig. 20). In this case, the moving dislocation can also dissociate in the plane of the stacking fault but is a Frank sessile dislocation and a Shockley partial. The loop is then separated into two parts. The stacking fault is swept away in only one of the parts and the dislocation line acquires a large jog that may move by prismatic glide.

Figures 6 to 10 show foils of quenched and aged aluminum containing loops of the type $\frac{a}{3}$ <111>. A few dislocation lines have moved during observation leaving several slip traces. Instead of straight edges, the slip traces exhibit indentations whose width is rather constant (300 to 500 Å) and whose length ranges from 200 to 1000 Å. Observation of two consecutive

pictures shows that a loop has been destroyed by the moving dislocation whenever an indentation in the slip trace appears. The indentation in the trace and the original position of the loop that is swept away generally are related by the direction AC.

Short cross-slip (500 Å to 1000 Å in projection) are also observed and exhibit rounded corners.

These results can be interpreted as interaction of the moving dislocation with a loop, followed by prismatic glide of part or all of the large jogs acquired by the dislocation. In this interpretation, the observed indentations or cross-slip traces are simply the intersection of the glide prism of the dislocation with the surface of the foil. The glide prism being parallel to a <110> direction, its intersection by a (110) plane shows an apparent length equal to $\frac{1}{\cos 60^\circ}$ = 2 times its width.

Intersections resulting in a protrusion on the slip-trace have never been observed. This may be explained by the fact that loops are all of the vacancy type and the stresses acting on the moving dislocation are compressions since they are due to local heating or carbon deposit in the region of observation. Therefore, the deformation of the foil due to moving dislocation is of the type shown in figure 18. An absorption of vacancies by the dislocation will always result in indentations on the slip trace and never in a protrusion.

In order to interpret particular observed interactions, the Burgers vector of the moving dislocation must be known. It can be determined by using certain features of the slip trace and the known orientation of the crystal. For example, the Burgers vector of the dislocation at L in figure 12 can be determined as follows: From the orientation and width of its trace its glide plane is d. Therefore, the Burgers vector is $\pm\vec{BA}$, $\pm\vec{AC}$ or $\pm\vec{BC}$. BC is not likely because it lies in the plane of the foil;

the resolved shear stress due to tension or compression would be zero. The short cross-slip 'R-R' in figure 13 shows that the other glide plane is b, which means that the Burgers vector must be $\pm\vec{AC}$.

Considering all the possible Burgers vectors and glide planes for the moving dislocation and the Frank loop, the observed interactions may be classified as follows:

1. The loop is lying on one of the glide planes of the moving dislocation:

Let AC be the direction of a dislocation in pure screw orientation (figure 19).and let loops lie on plane b or plane d. There is no attraction between the loop and the moving dislocation since their Burgers vectors are perpendicular (βB and δD perpendicular to AC).

a) the loop lies on the active glide plane: Let d be the active glide plane of the moving dislocation and let a Frank loop lie on this plane with Burgers vector δD (figure 19). If the dislocation intersects the loop, the dislocation AC will split into two partials:

$$AC \rightarrow A\delta + \delta C$$

which will combine separately with δD:

$$A\delta + \delta D \rightarrow AD$$

$$C\delta + \delta D \rightarrow CD$$

If the dislocation line is then pulled away from the loop, the result of the interaction is to change the loop from a Frank sessile loop to one of the perfect prismatic type. The probability of such an event is very small since the dislocation is moving parallel to the plane of the loop.

This interaction apparently has taken place where the dislocation L, seen on the left of the picture in figure 12, passed by loop M, seen in good contrast in figure 12. The slip trace left by the dislocation L moving to the right of the picture can be seen in figure 13 where M' is now hardly visible and gives rise to a double image of type (( )).

As pointed out by Yoshida[16] it may not be necessary for the dislocation to move exactly in the actual plane of the loop. By passing only a few interatomic distances away from the loop, the stress field of the dislocation may induce the nucleation of a Shockley partial inside the Frank loop. This remote interaction may explain why this transformation is often observed although very improbable from the purely geometrical point of view.

b) the loop lies on the inactive glide plane of the moving dislocation:

Let d be the active glide plane and the Frank loop lie on b with Burgers vector βB (figure 20). This case has a higher probability of occurring from the purely geometrical point of view. The moving dislocation will get two nodes and will be pinned. Unless one arc of the loop is caused to glide by the same stress as that acting on the moving dislocation, the loop will be passed by bowing out of the moving dislocation on either side. As in case a), a perfect loop is left. Assuming BC will glide, then a smaller perfect prismatic loop of Burgers vector BA would be left behind.

This mechanism may explain the interaction observed in figure 14a, b, c. Loop R of figure 14a gives rise to an indentation R_1, in the slip trace plus a loop R_2 of smaller size (figure 14b). On figure 14c, R_2 is still visible but in position R'_2 after prismatic glide along the expected direction, i.e., parallel to BC. This glide was probably caused by the close passage of a second dislocation which, from its trace, can be seen to have moved in plane d.

2. The loop does not lie on either glide plane of the moving dislocation:

Let BC be the direction of a dislocation in pure screw orientation (figure 21) and let loops lie on plane b with Burgers vector βB. The interactions in this case are as follows:

The moving dislocation can split on contact with the loop according to the reaction:

$$BC \rightarrow B\beta + \beta C$$

and the Shockley partial βC will sweep out the stacking fault on one half of the loop, whereas the Frank sessile $B\beta$ will close the second half into a smaller Frank sessile loop. The moving dislocation can then go on moving but is now dragging a segment that loops out of the original glide plane. The Burgers vectors of the moving dislocation and of the loop are not at right angles. For small loops, as in the present case, this may cause local cross-slip of the moving dislocation towards the edge of the loop which attracts it. The stacking fault is then completely swept out; no part of the loop is left behind. This mechanism accounts for the interactions observed in figure 12-13 from N and Q. These are loops of different type but have symmetrical orientations with respect to the moving dislocation. After interaction as shown by figure 13, the loops are gone and indentations N' and Q' have been produced on the slip trace of the moving dislocation where the segment of line looping out of the original glide plane has slipped to the surface along direction AC.

If the loop does not intersect the active slip plane of the moving dislocation but is close enough to attract it (figure 22), the dislocation may cross-slip and interact with the loop. An extra-large pair of jogs is created and may account for the exaggerated indentations observed in F' and G' (figure 8) originating from loops F and G (figure 7).

If the loop does intersect the active slip plane of the moving dislocation, local cross-slip may occur but would involve the formation of dipoles J_1 and J_2 (figure 23). This case should involve both protrusions and indentations on the slip trace. It was not observed experimentally.

This type of interaction seems also to favor the total cross-slip of the moving dislocation. The two large jogs created by interaction with a loop may be driven in opposite directions in the cross-slip plane by the applied stress. In this case, the whole dislocation is moved off of its original glide plane by a distance about equal to the diameter of the loop. This explains the interaction with loop P (figure 12). The two jogs reaching opposite surfaces of the foil produce offsets, P' and P".

Other interactions are visible on figure 12-13 and figures 7-10. They give rise to both indentations and debris but involve more than one loop at a time. They cannot be classified according to the above described interactions and have not been interpreted.

IV. CONCLUSIONS

1. Quenching high purity aluminum from 650°C into water at 0°C results in the formation of colonies of loops as in polycrystalline material. The loops have an average diameter of 250 Å and the colonies contain about 6×10^{14} loops/cm^3.

2. Electron diffraction contrast experiments show that approximately 99% of the loops are of the Frank sessile type; an $\frac{a}{3}\langle 111\rangle$ dislocation enclosing an intrinsic stacking fault.

3. Frank loops interact with moving dislocations in three different ways that all lead to a change in the Burgers vector of the loop from $\frac{a}{3}\langle 111\rangle$ to $\frac{a}{2}\langle 110\rangle$. The moving dislocation may acquire large jogs that can glide to the surface of the foil on the cross-slip plane resulting in indentations on the slip trace or transfer of the moving dislocation to a new glide plane about one loop diameter to one side of the original glide plane.

Acknowledgments

The author expresses his gratitude to Professor Jack Washburn for his continued interest and encouragement and to him and Professor Gareth Thomas for helpful discussions. This work was done under the auspices of the United States Atomic Energy Commission through the Inorganic Materials Research Division of the Lawrence Radiation Laboratory.

References

1. D. Kuhlmann-Wilsdorf and H. G. F. Wilsdorf, J. Appl. Phys., 31, 516 (1960).

2. F. J. Bradshaw and S. Pearson, Phil. Mag., 5, 24 (1960).

3. C. Panseri and T. Federighi, Phil. Mag., 3, 1223 (1958).

4. W. De Sorbo and D. Turnbull, Acta Met., 7, 83 (1959).

5. M. Meshii and J. W. Kauffmann, Acta Met., 7, 180 (1959).

6. R. Maddin and A. H. Cottrell, Phil. Mag., 46, 735 (1955).

7. T. Kino, J. Sci. Hiroshima Univ., 22, 259 (1958).

8. F. C. Frank, Symposium on the Plastic Deformation of Crystalline Solids, (Carnegie Institute of Technology, Pittsburgh, 1950) O.N.R., p. 150; and Deformation and Flow of Solids (Berlin: Springer,1956) p. 73.

9. F. Seitz, Phys. Rev., 79, 890 (1950).

10. J. Silcox and P. B. Hirsch, Phil. Mag., 4, 72 (1959).

11. P. B. Hirsch, J. Silcox, R. E. Smallman and K. H. Westmacott, Phil. Mag., 3, 897 (1958).

12. R. Vandervoort and J. Washburn, Phil. Mag., 5, 21 (1960).

13. R. L. Segall and R. M. J. Cotterill: Reported by P. B. Hirsch, International Conference on Magnetism and Crystallography, Kyoto (1961) 11, p. 143.

14. S. Yoshida, Y. Shimomura and M. Kiritani, J. Phys. Soc. Japan, 17, 1196 (1962).

15. G. Saada, Acta Met., 10, 551 (1962).

16. S. Yoshida, M. Kiritani and Y. Shimomura, J. of Phys. Soc. Japan, 18, 175 (1963).

17. M. J. Whelan and P. B. Hirsch, Phil Mag., 2, 1121 (1957); and Phil. Mag., 2, 1303 (1951).

18. N. Thompson, Bristol Conference,(London, 1955).

19. A. Howie and M. J. Whelan, Proc. Roy. Soc., A263, 277 (1961).

20. A. Howie and M. J. Whelan, Proc. Roy. Soc., A267, 206 (1962).

21. R. Gevers, Phil. Mag., 7, 50 (1962).

22. E. Ruedl, P. Delaviguette and S. Amelinckx,"Radiation Damage in Solids" Part I (1962) p. 363.

23. J. Takamura, J. of Applied Physics, 33, 247 (1962).

24. R. Welsh, J. of Institute of Metals, 85, 129 (1956).

25. J. D. Embury, C. M. Sargent and R. B. Nicholson, Acta Met., 10, 1118 (1962).

26. F. Vincotte, Master's Thesis, Lawrence Radiation Laboratory, University of California, Berkeley (1962).

27. R. B. Nicholson, Report of International Conference on Structure an Properties of Thin Films (Bolton Landing, New York, 1959) p. 193.

28. G. Thomas, Phil. Mag., 4, 606 (1959).

29. P. B. Hirsch and J. Silcox, Growth and Perfection of Crystals, Proc. International Conf. on Crystal Growth (New York, 1958) p. 262.

30. J. Washburn and G. Saada, University of California Lawrence Radiation Laboratory report 10427. (August 1962)

31. D. Kuhlmann and Wilsdorf, Phil. Mag., 3, 125 (1958).

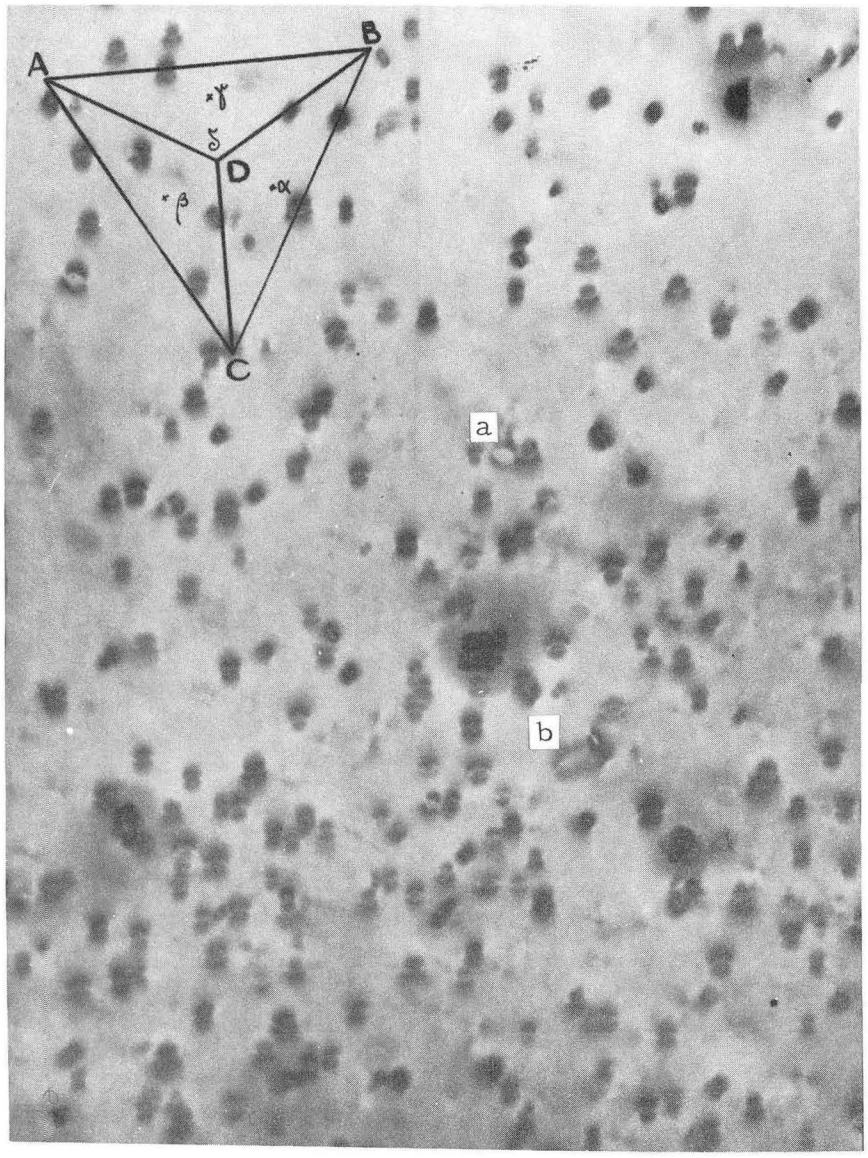

Fig. 1a(X 70,000)

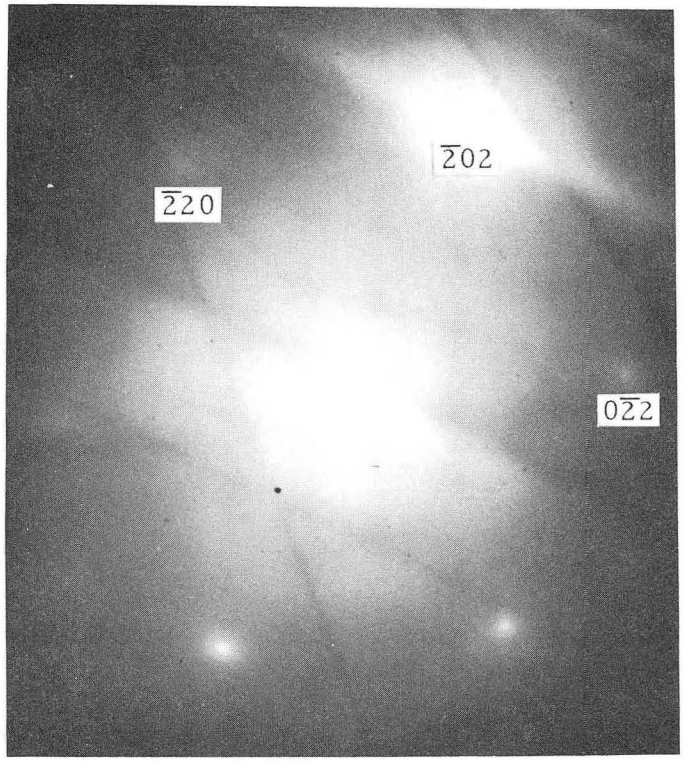

Fig. 1b

Diffraction conditions:

$\vec{b}$	$\vec{g}:\bar{2}02$	contrast
$1/3[\bar{1}11]$ or γC	4/3	in contrast
$1/3[1\bar{1}1]$ or αA	0	out of contrast
$1/3[11\bar{1}]$ or βB	-4/3	in contrast

ZN-3774

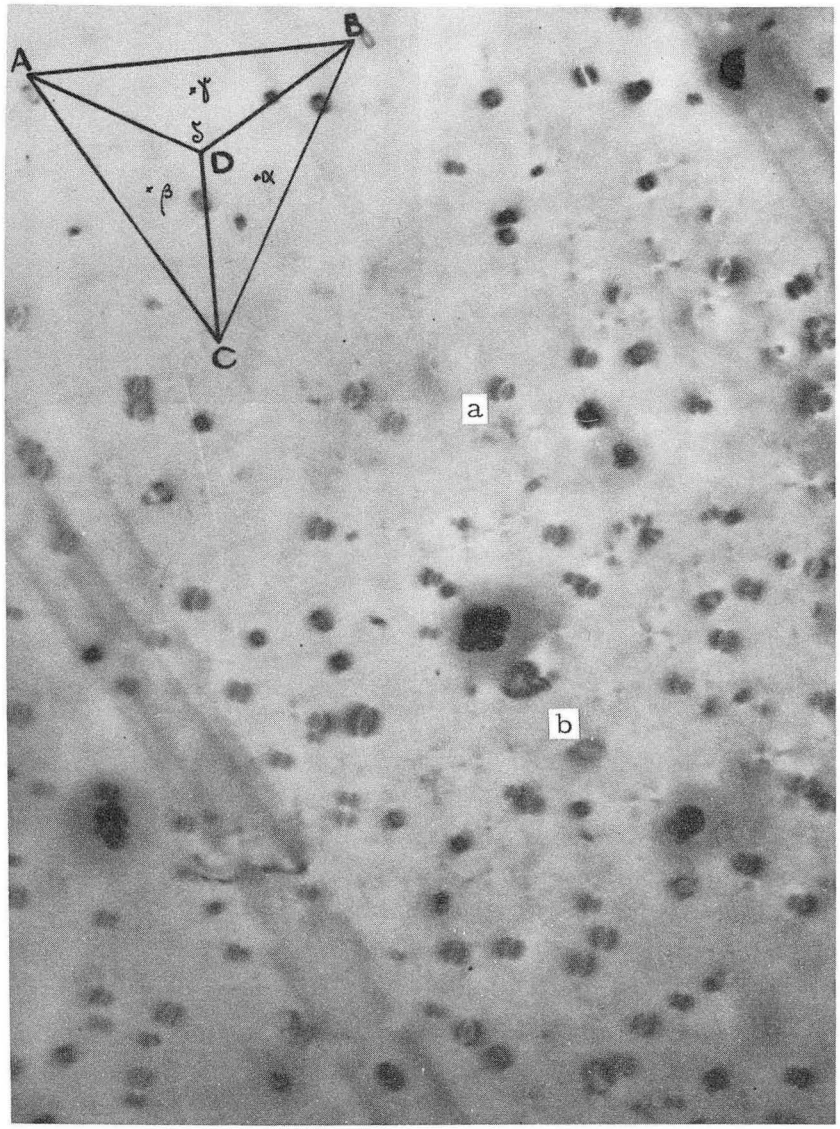

Fig. 2a(X 70,000)

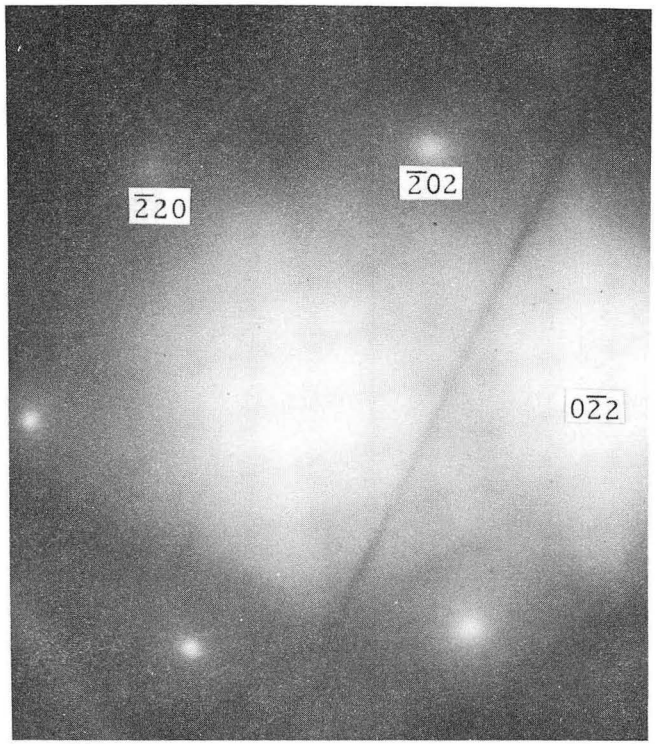

Fig. 2b

Diffraction conditions:

$\vec{b}$	$\vec{g}: 0\bar{2}2$	contrast
$1/3[\bar{1}11]$ or γC	0	out of contrast
$1/3[1\bar{1}1]$ or αA	4/3	in contrast
$1/3[11\bar{1}]$ or βB	-4/3	in contrast

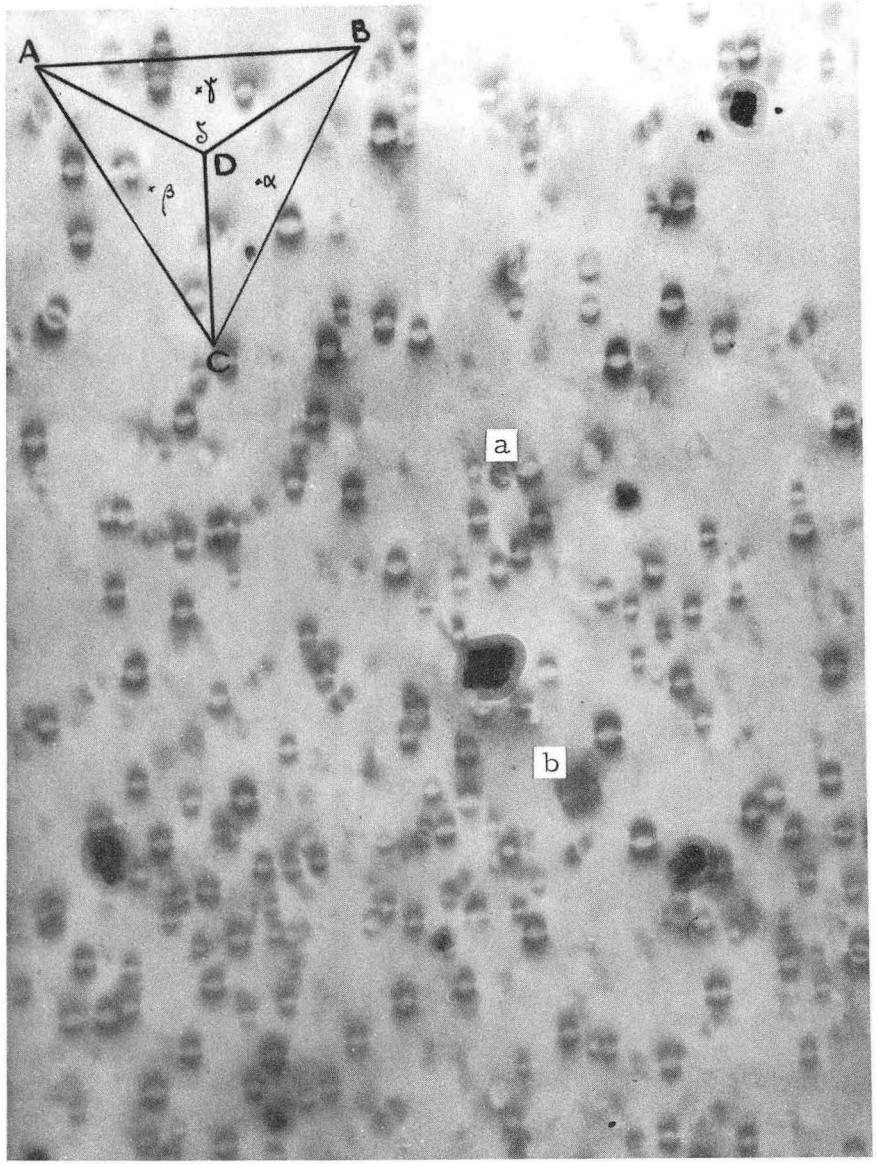

Fig. 3 (X 70,000). Same region as in Fig. la and 2a with the set of loops of γC type in good contrast. Note that loops a and b are visible on all three pictures (perfect prismatic loops). Note on Fig. la and lb the relation between the position of the image of loop (inside the loop or outside) with the sign of the product $\vec{g}.\vec{b}$.

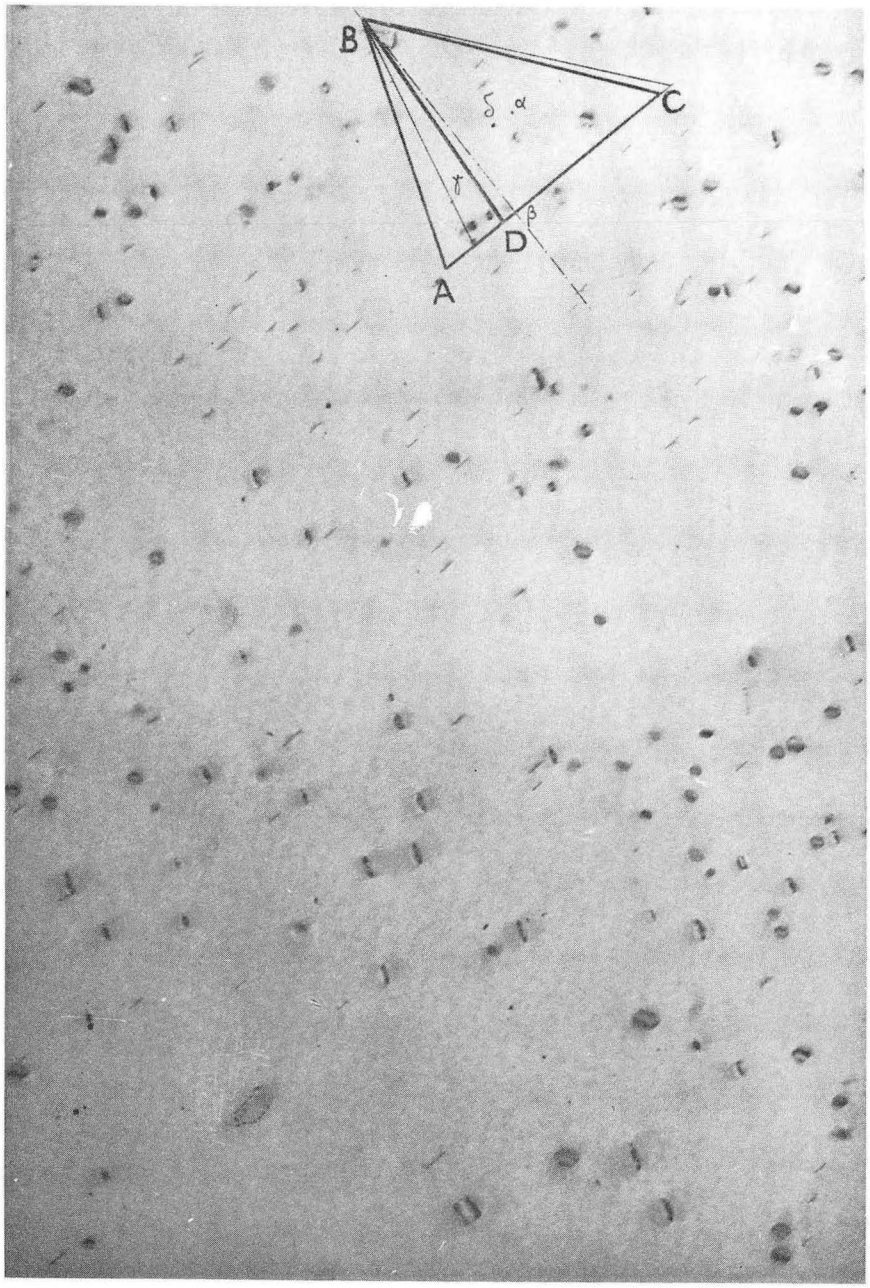

Fig. 4 (X 50,000). High purity aluminum quenched from 651°C into water at 1°C. Orientation close to [110]. All four sets of Frank sessile loops are visible.

ZN-3777

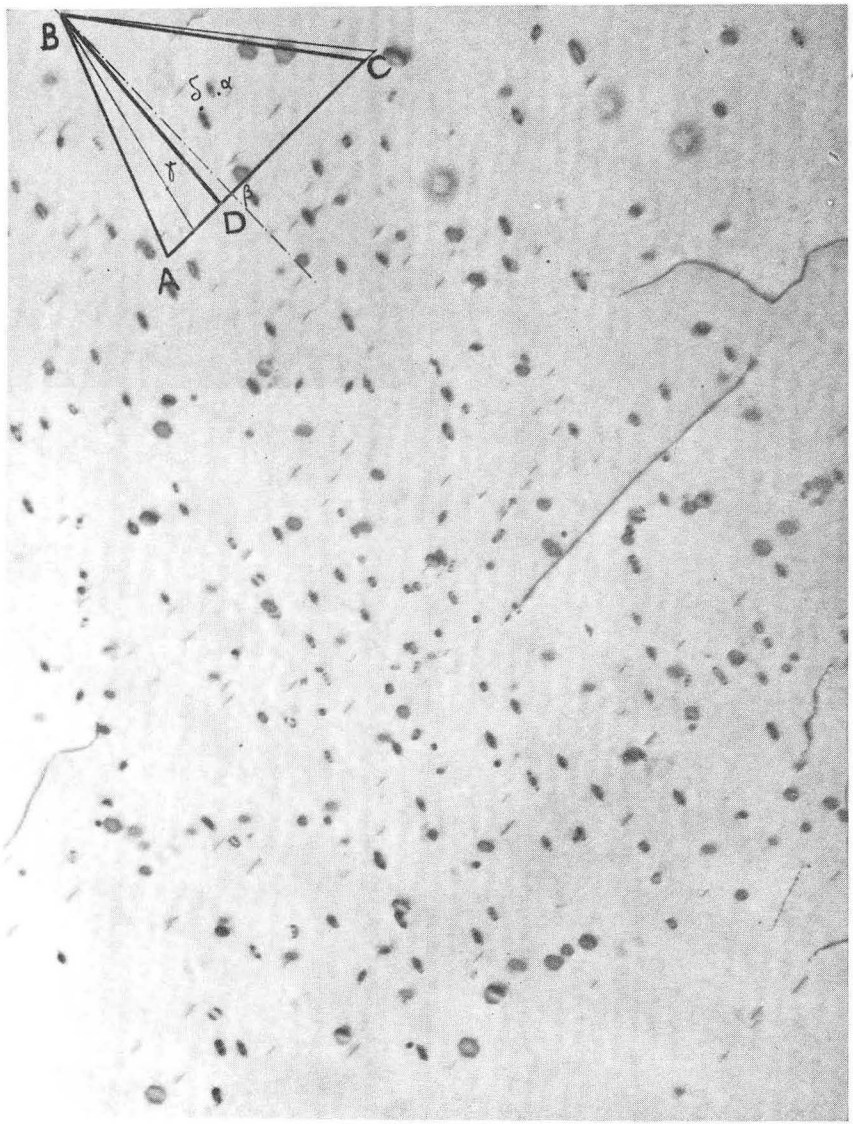

Fig. 5. (X 50,000).

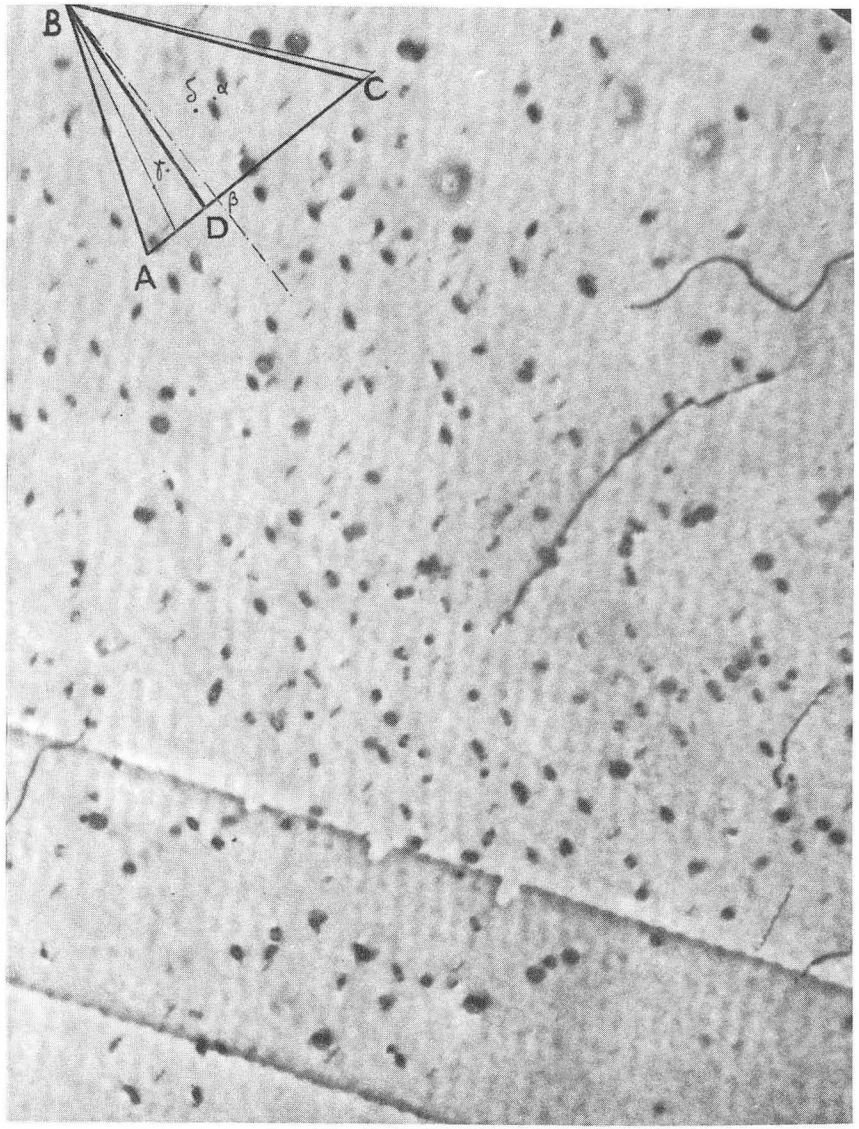

Fig. 6. (X 50,000).

ZN-3778

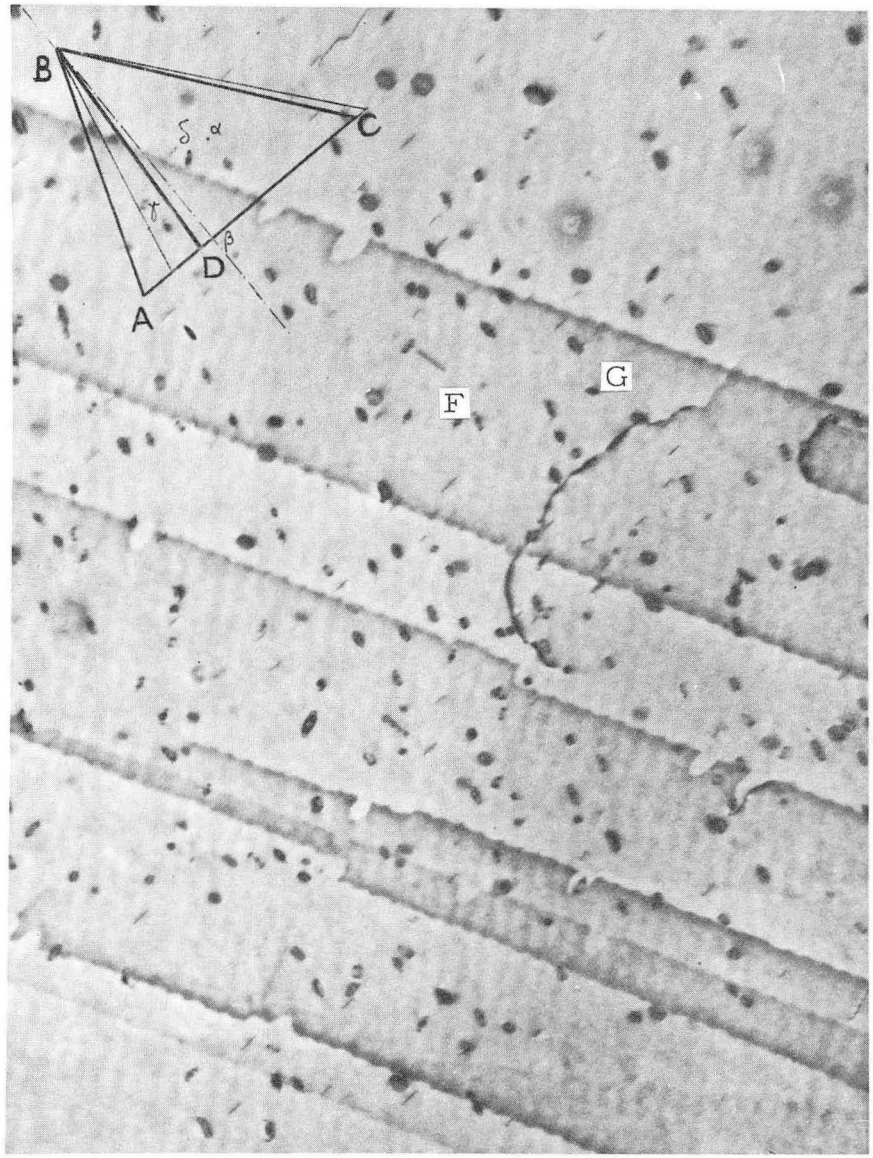

Fig. 7. (X 50,000).

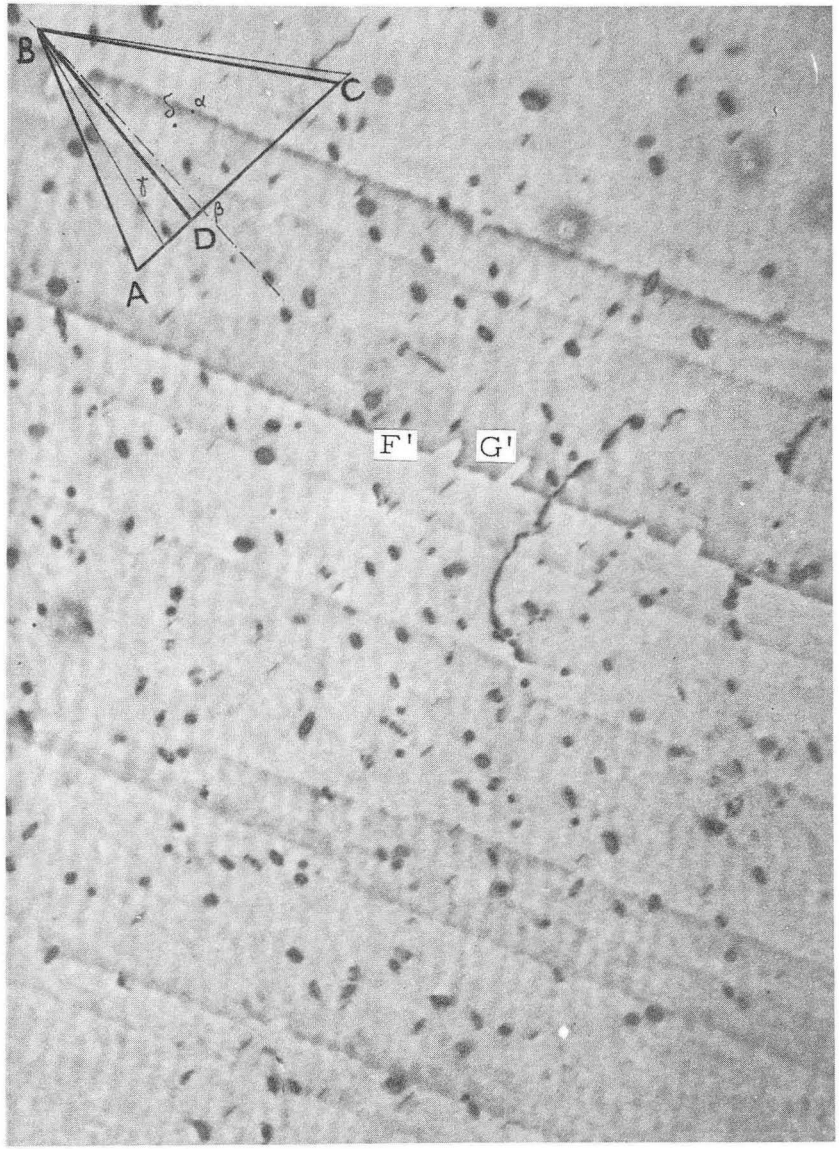

Fig. 8. (X 50,000).

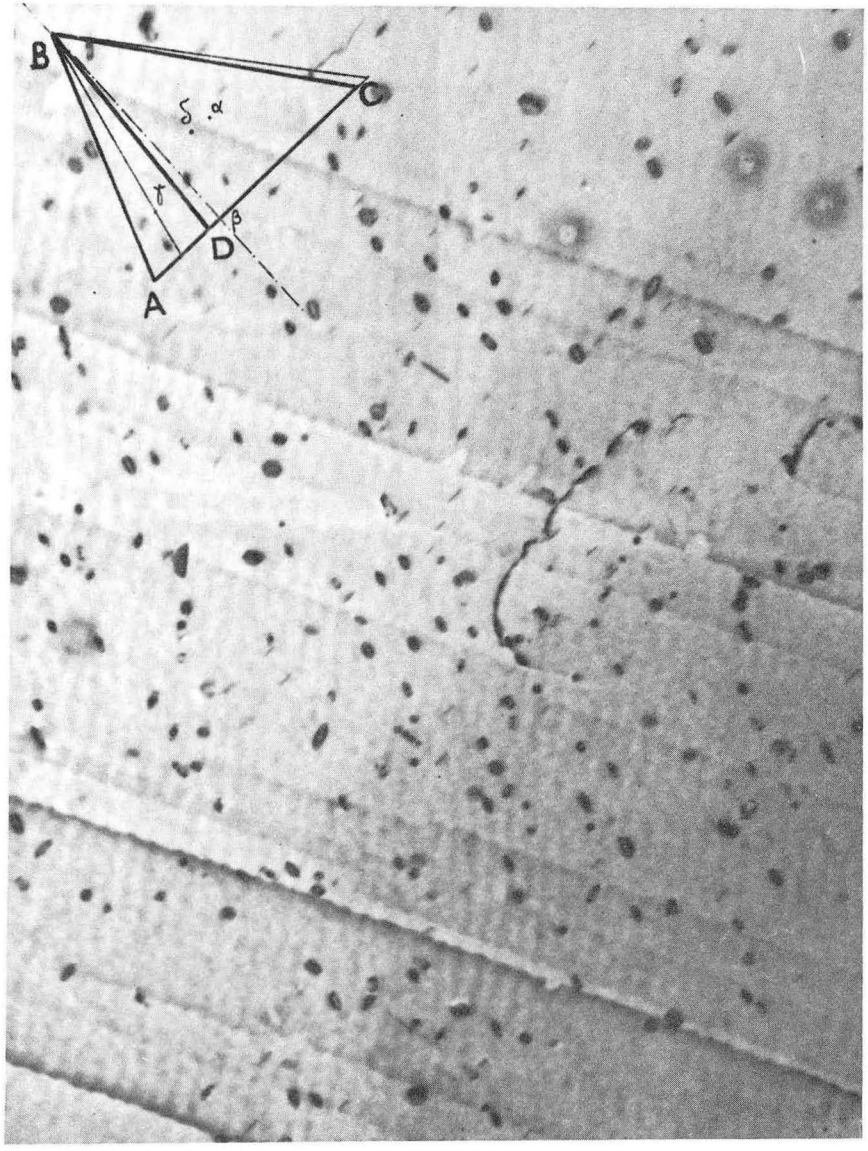

Fig. 9. (X 50,000).

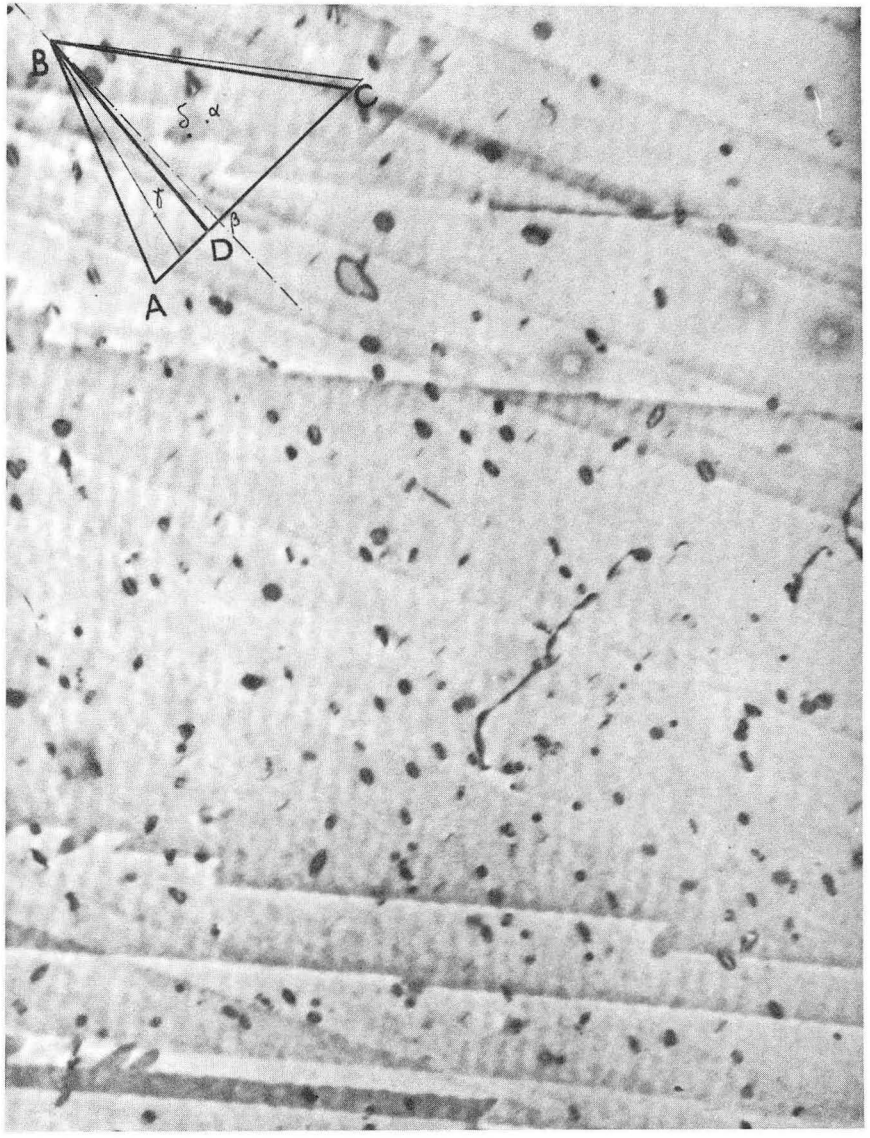

Fig. 10. (X 50,000).

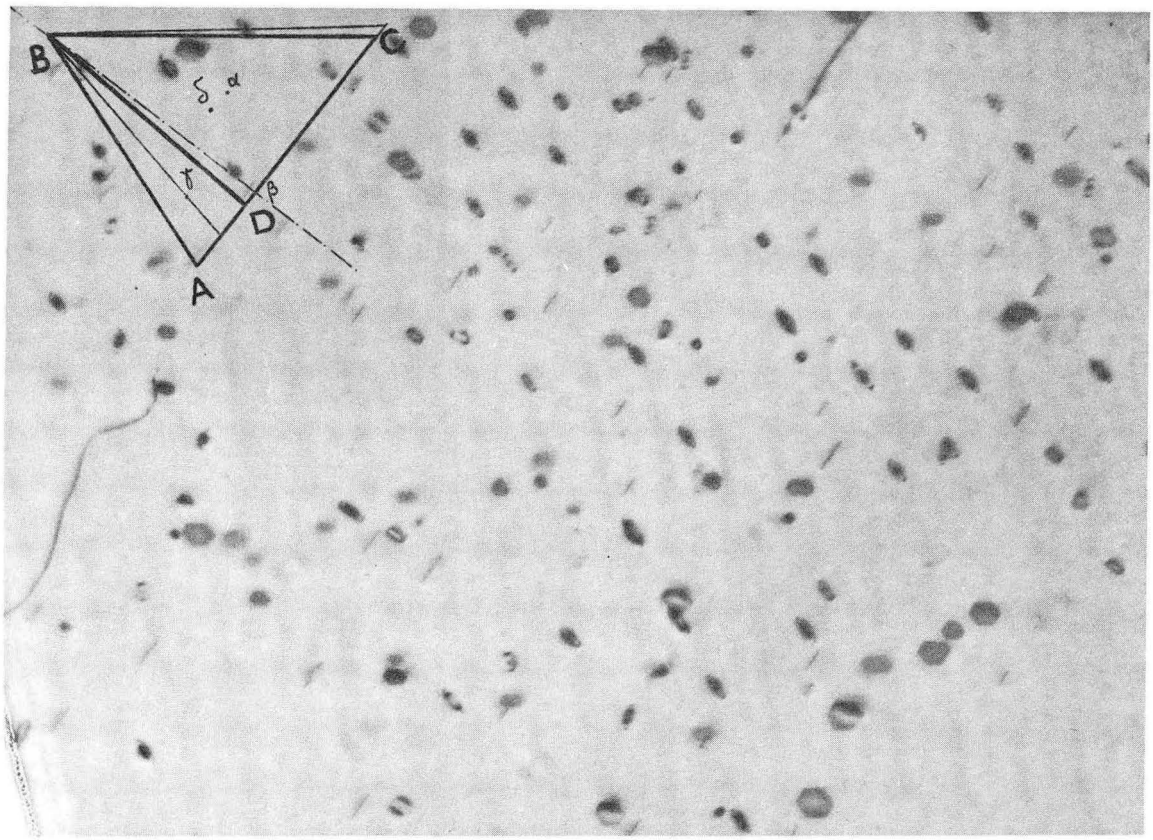

Fig. 11 (X 80,000). Detail of Fig. 5. Orientation close to [110]. Note that the four sets of loops are visible.

ZN-3781

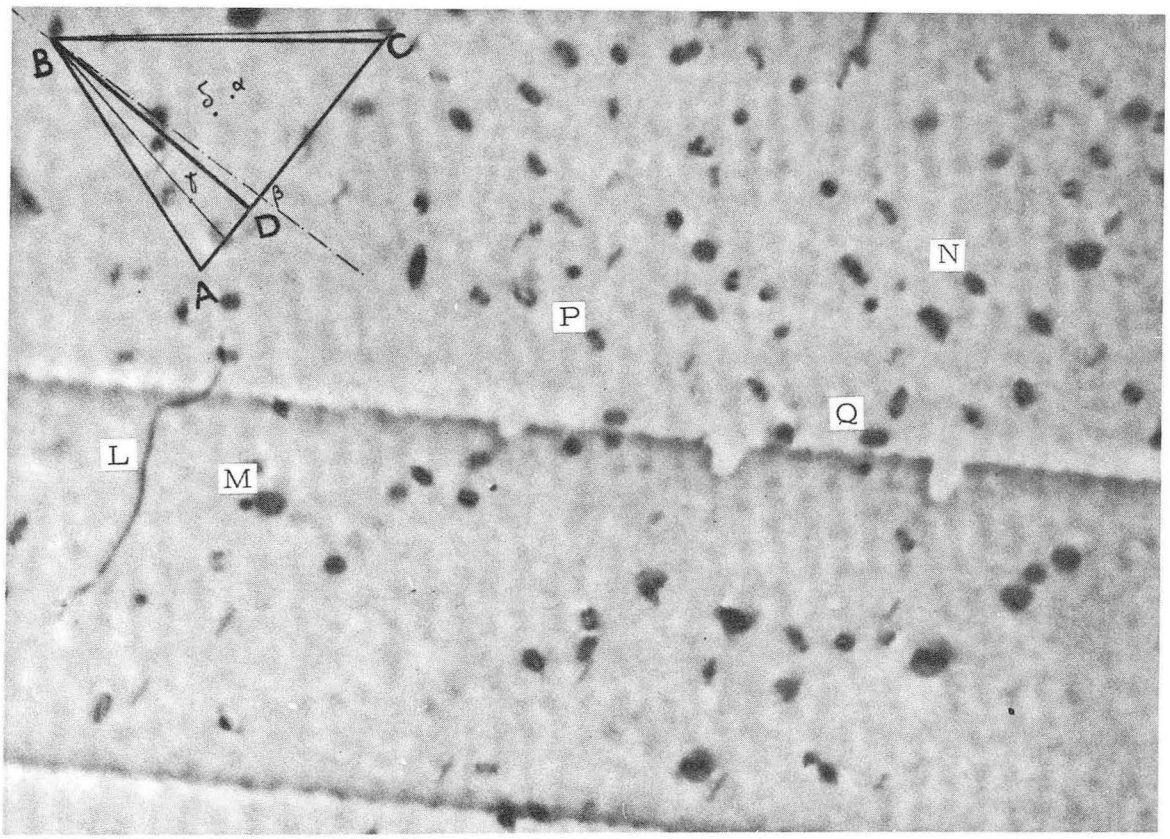

Fig. 12 (X 80,000). Detail of Fig. 6. Note dislocation L in almost pure screw orientation. Loops M, N, P and Q give rise to interactions with moving dislocations (see Fig. 13).

ZN-3782

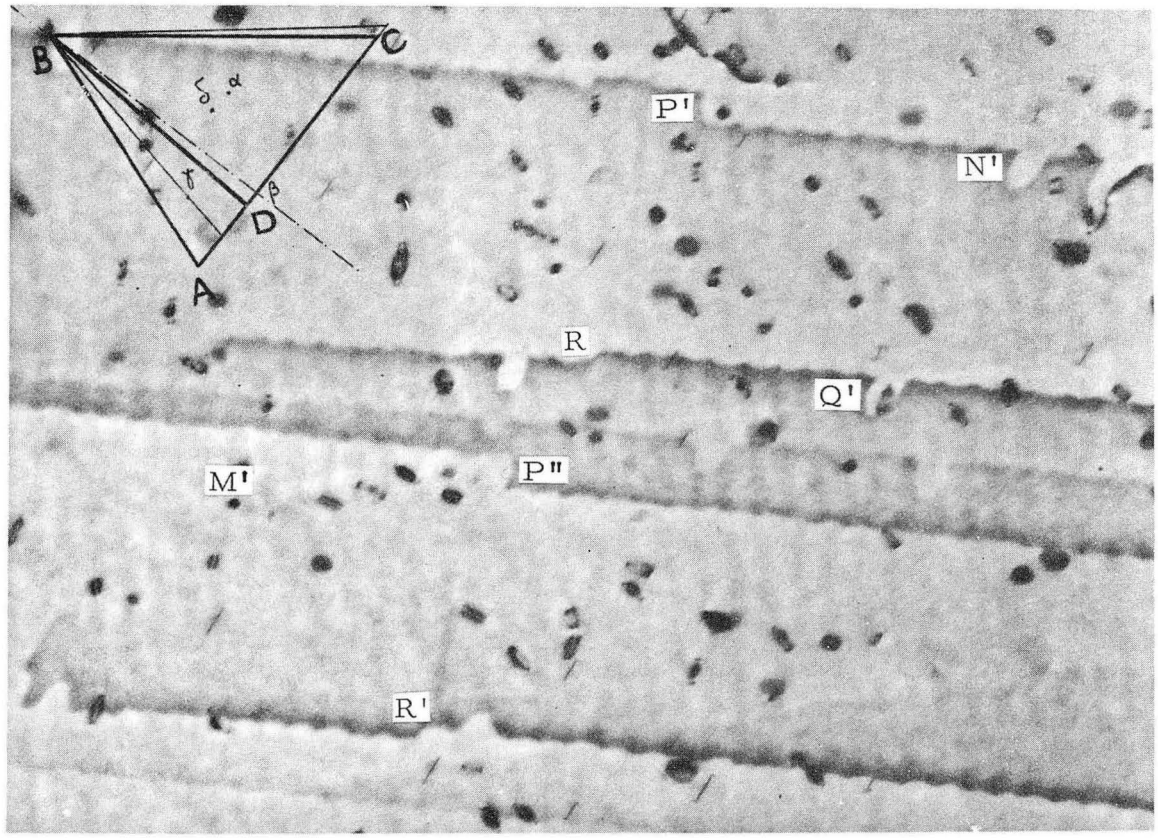

Fig. 13 (X 80,000). Interaction between a dislocation line L and a Frank loop M lying on its acting glide plane. Interaction between a dislocation line and Frank loops N and P (Fig. 12) not lying on any of its glide planes. Traces resulting from interactions are seen in N' and P'P".

ZN-3783

(a)

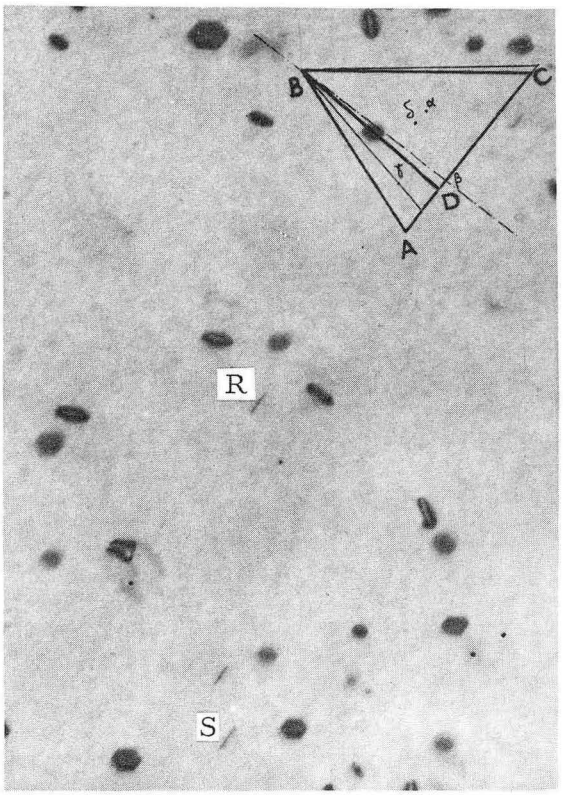

(b)

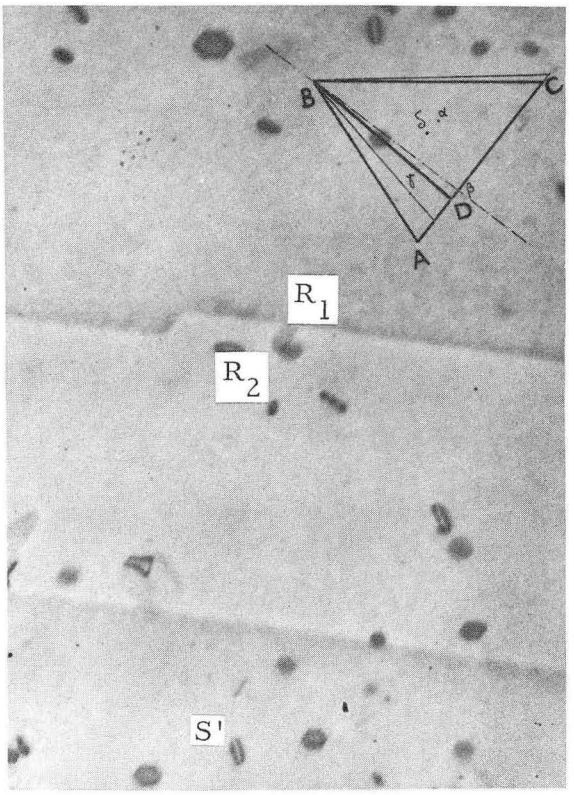

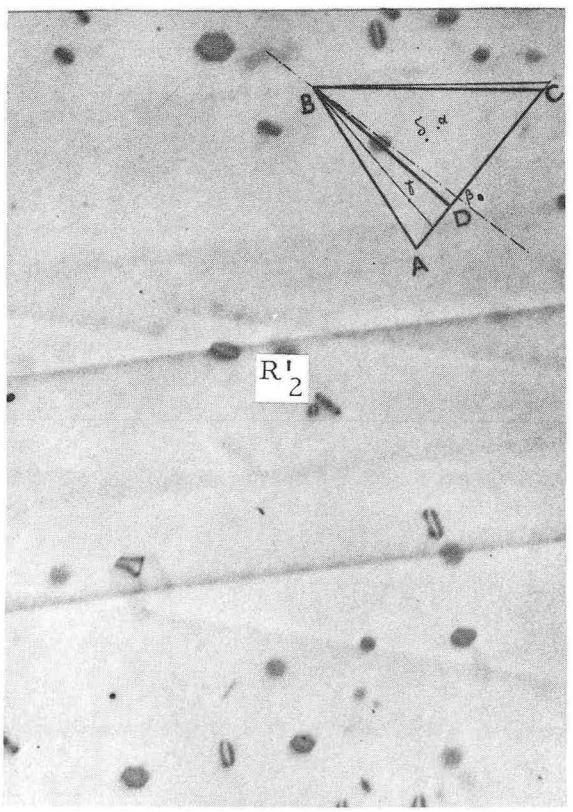

(c)

Fig. 14 a, b and c (X 60,000). Interaction between a moving dislocation and a Frank loop R not lying on its acting glide plane. Residue R_2 is seen moving along the direction BC.

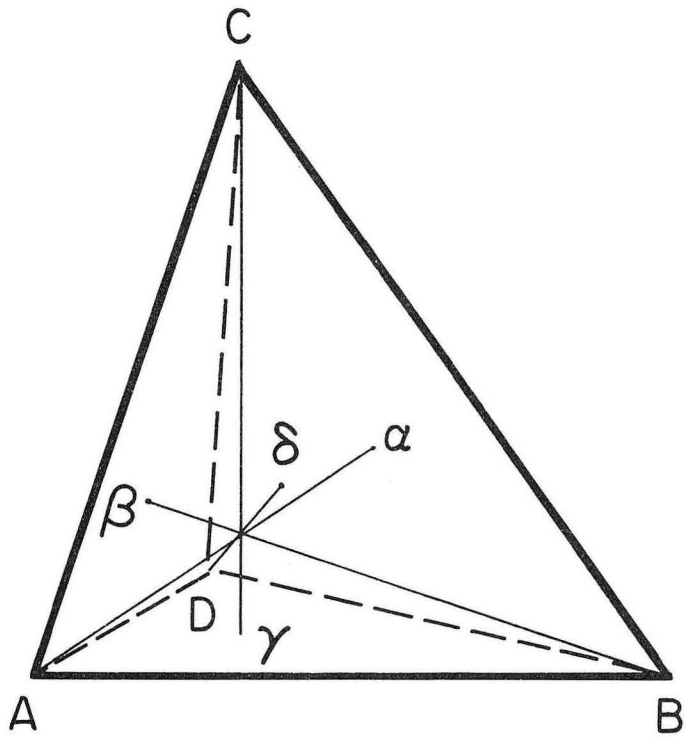

MU-30933

Fig. 15. Thompson tetrahedron.

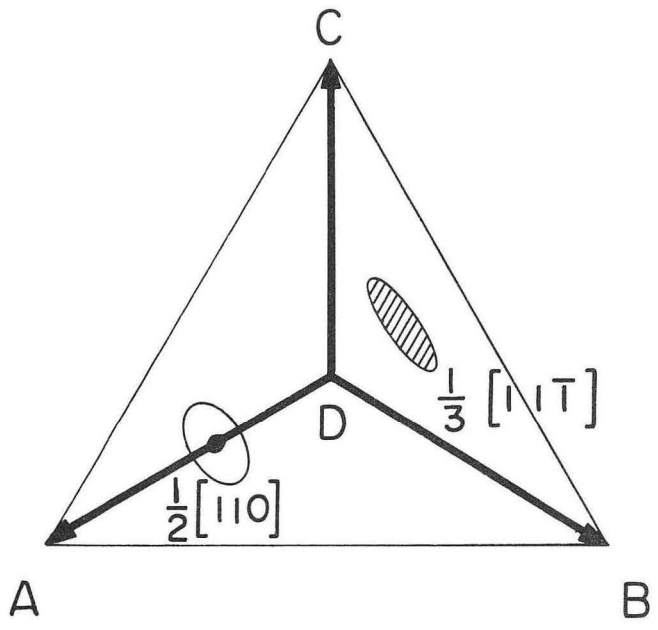

MU-30934

Fig. 16. Frank sessile loop $1/3[11\bar{1}]$ and perfect prismatic loop $1/2[100]$ elongated along the same direction BC. [In projection on the (111) plane.]

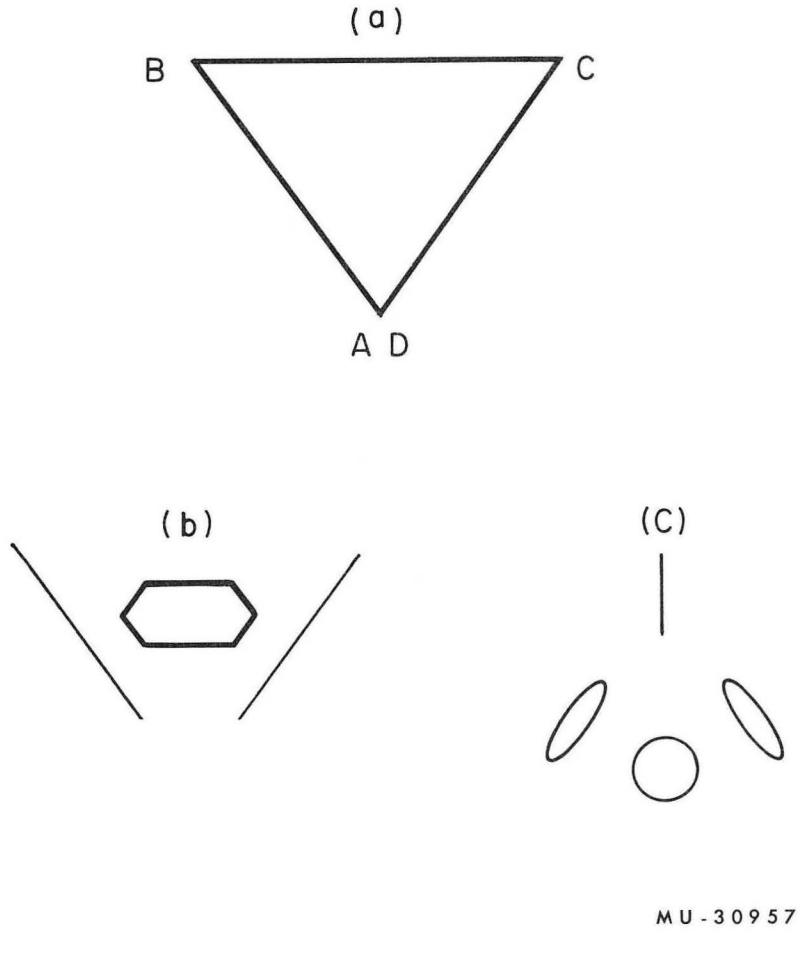

Fig. 17. (a) Thompson tetrahedron with edge AD perpendicular to the plane of the figure. (b) Aspect of Frank sessile loops in a foil with [110] orientation. (c) Aspect of perfect prismatic loops in the same direction of observation.

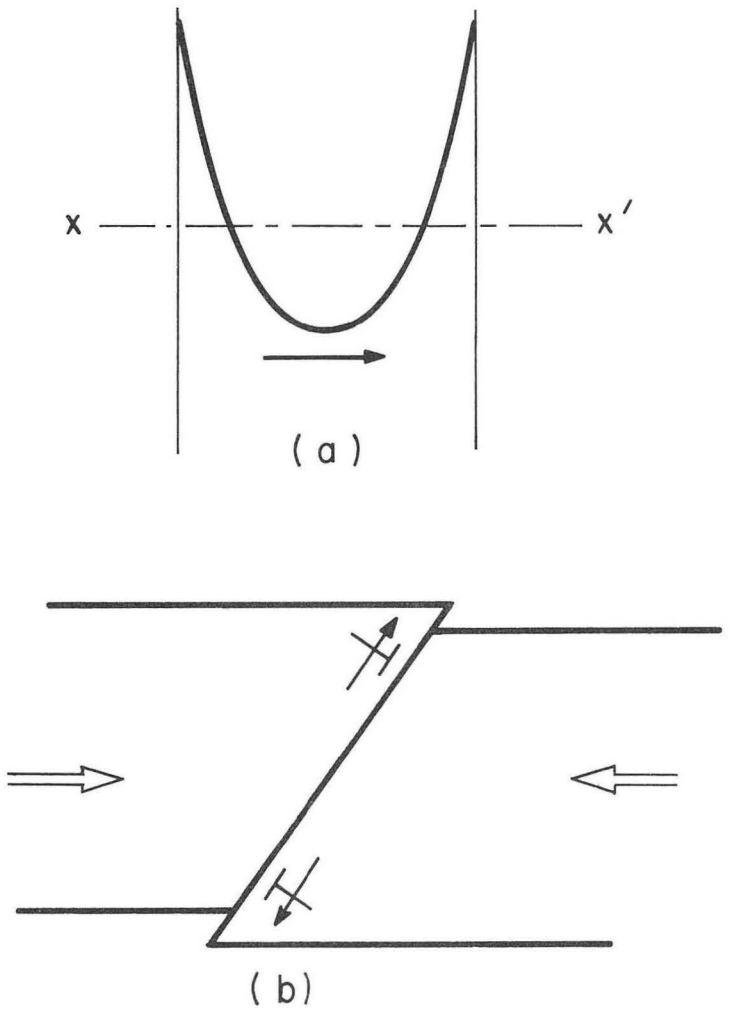

Fig. 18. (a) Moving dislocation and its slip trace.
(b) Section view in plane xx'.

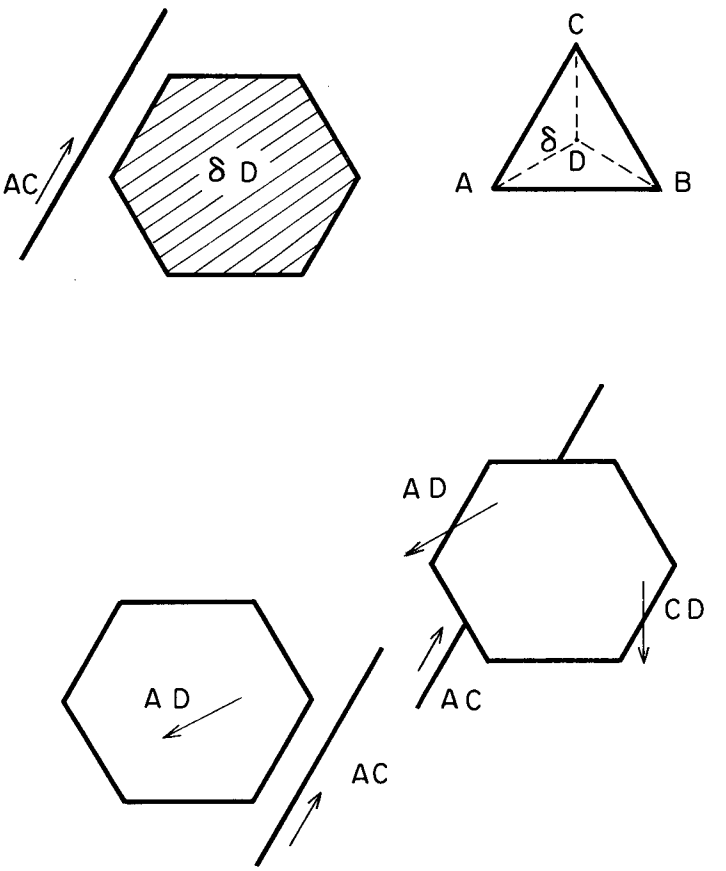

Fig. 19. Interaction between a moving dislocation $\vec{AC}$ and a Frank sessile loop lying on its acting glide plane.

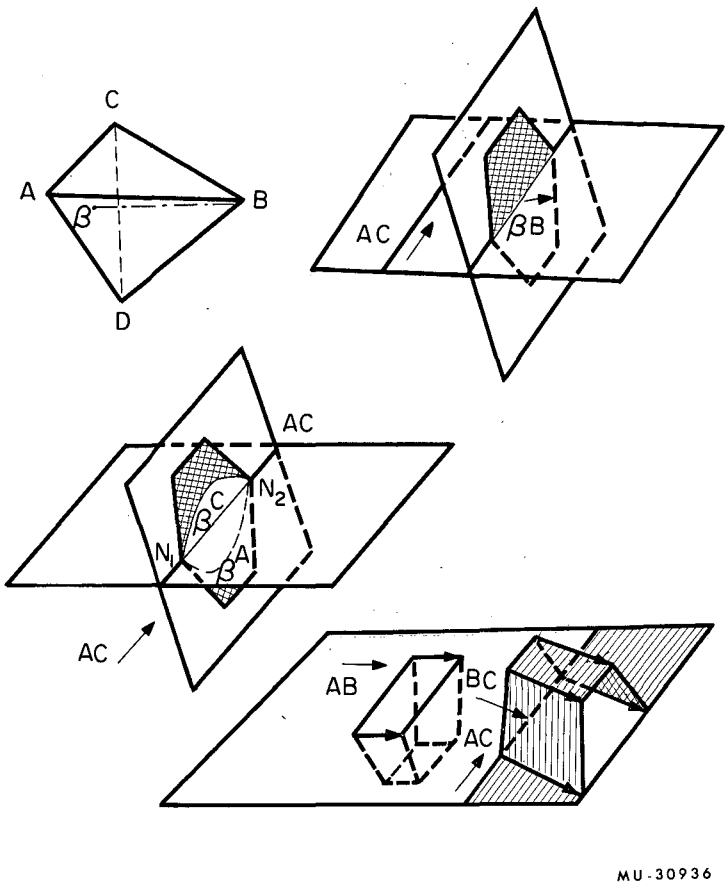

Fig. 20. Interaction between a moving dislocation $\vec{AC}$ and a Frank sessile loop lying on one of its glide planes.

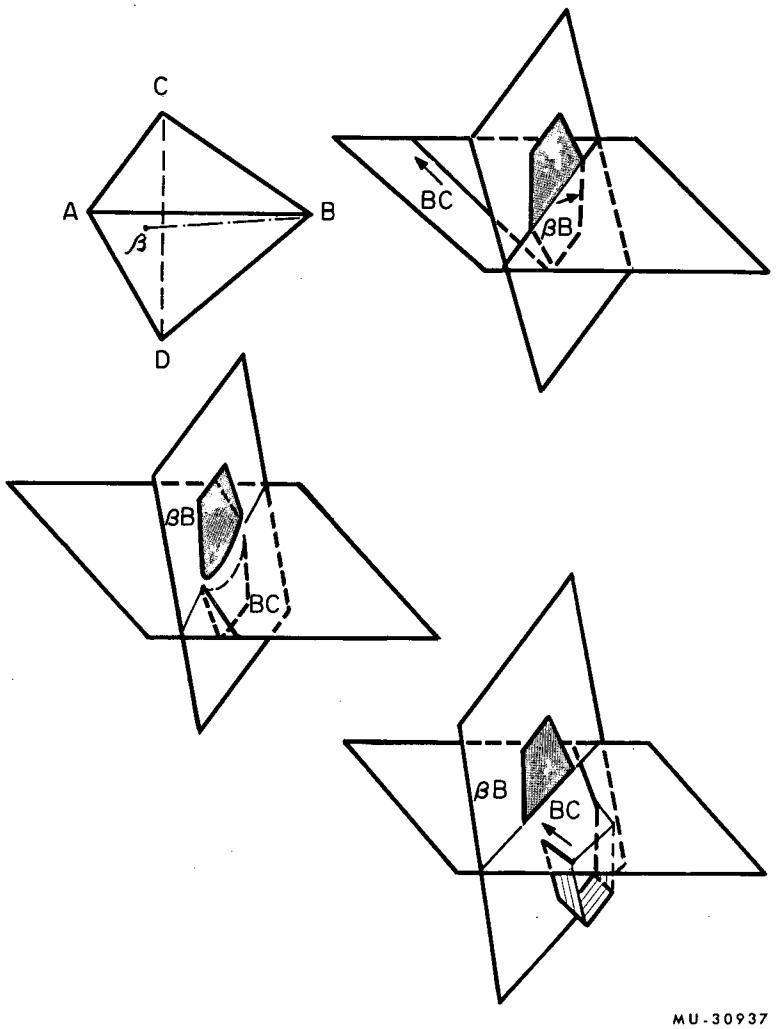

Fig. 21. Interaction between a moving dislocation $\vec{BC}$ and a Frank sessile loop not lying on either of its glide planes.

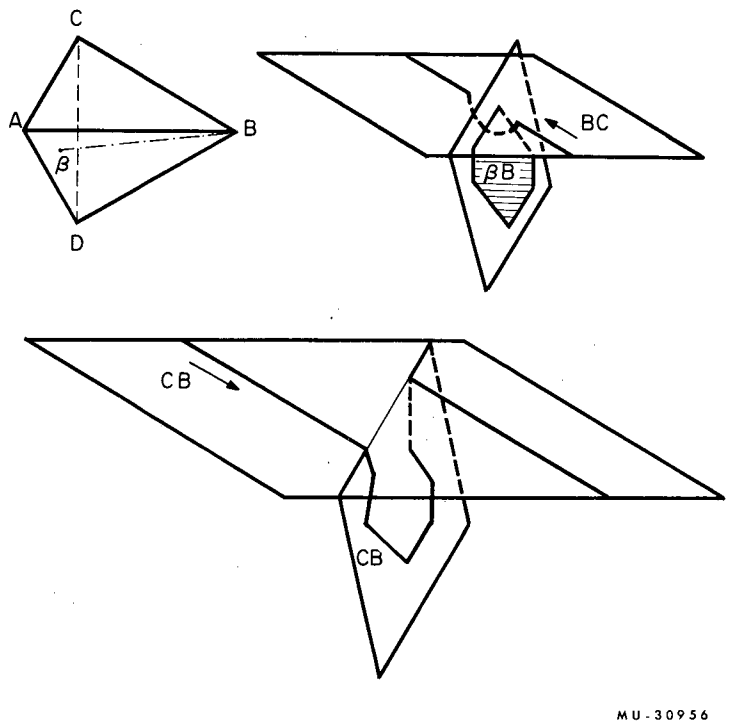

Fig. 22. Local cross-slip of dislocation $\vec{BC}$ causing exaggerated indentations.

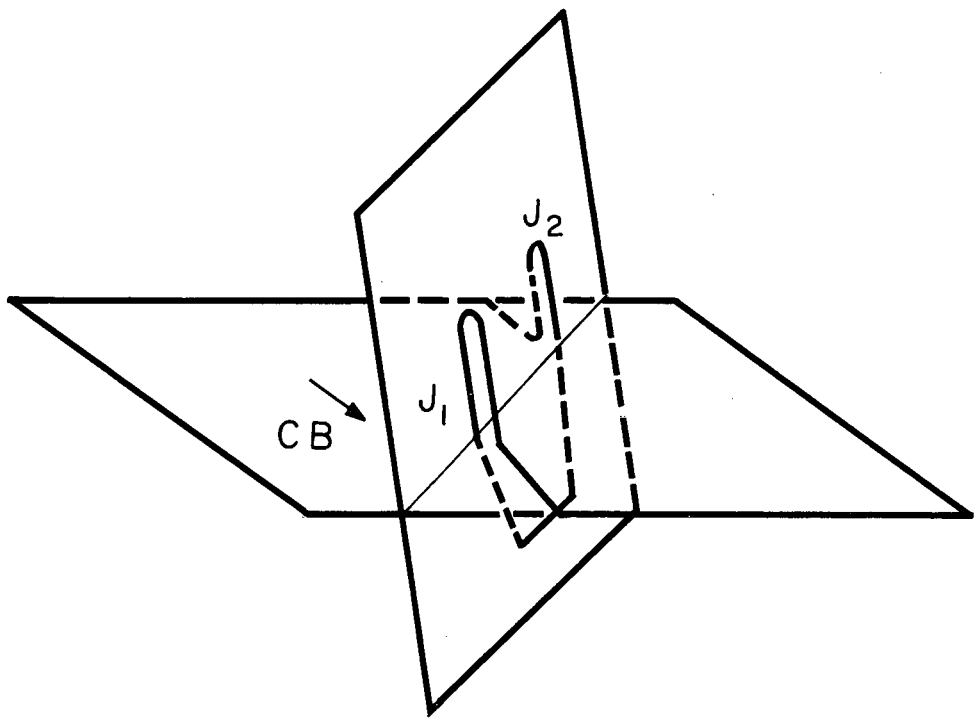

Fig. 23. Local cross-slip of dislocation $\vec{CB}$ when interacting with a small Frank sessile loop.